Available online at www.sciencedirect.com
ScienceDirect
Polymer 48 (2007) 1058–1065
polymer
www.elsevier.com/locate/polymer

Reactive compatibilization of PE/PS blends. Effect of copolymer chain length on interfacial adhesion and mechanical behavior

Mónica F. Díaz, Silvia E. Barbosa*, Numa J. Capiati

Planta Piloto de Ingeniería Química, PLAPIQUI (UNS-CONICET), Cno. La Carrindanga Km 7, 8000 Bahía Blanca, Argentina

Received 25 October 2006; received in revised form 20 December 2006; accepted 21 December 2006
Available online 27 December 2006

Abstract

This paper deals with in situ compatibilization of PE/PS blends via Friedel–Crafts reaction, performed at the interphase. Two polyethylenes having different molecular weights, and the same PS, were used along a wide range of catalyst concentration. The influence of the graft copolymer architecture and content on the efficiency of blend compatibilization was studied. The emulsifying effect, morphological aspects and mechanical behavior were also assessed for these blends. The amount of copolymer formed increases with catalyst concentration and the short chain length fraction of the homopolymers. The high molecular weight (MW) copolymers behaved as better compatibilizers as they showed, at the cmc, greater graft copolymer concentration than the low MW ones. A substantial increase in interfacial adhesion and particle size reduction was observed, even at catalyst concentrations as low as 0.3 wt%. In correspondence, mechanical properties, like ductility and yield strength, were enhanced by the effect of this Friedel–Crafts reaction's compatibilization.

Keywords: Reactive compatibilization; PE/PS blends; Friedel–Crafts alkylation reaction

1. Introduction

The melt-blending technique provides an easy and efficient way to generate polymeric materials with novel and targeted properties as well as to achieve a reasonable set of properties from plastic blends, without previous component separation (e.g. municipal-plastic wastes). Even though most of the blends are immiscible, the direct blending causes weak interphases limiting the ability to develop materials that can compete with engineering polymers [1–3].

In such heterogeneous systems, a satisfactory overall physical–mechanical behavior will critically depend on morphology and interfacial adhesion. In this sense, the mechanical properties of a multiphase system will be driven by the interphases' ability to transmit stresses from one phase to the other. The interphase was considered by many authors as a third phase in the blend, which has a thickness and properties different from those of the components, and needs to be compatibilized in order to enhance the blend properties [1–3]. The compatibilization processes are based on the improvement of adhesion between phases, the reduction of interfacial tension and the phase stabilization by the inhibition of droplet coalescence in subsequent manufacturing process [2–6].

The compatibilization of a blend is carried out either by adding a compatibilizer agent to the blend or producing the agent by an in situ reaction. In both processes the agent, which is located at the interphase, interacts with the phases by chain entanglement because of its physicochemical affinity to them. The reactive compatibilization is preferred as it seems to render more stable interphase products than those obtained by addition [7–9]. The in situ interfacial agent is formed from the same homopolymers that will be compatibilized. In this sense, it behaves as a ''tailor-made compatibilizer'', allowing a high physicochemical affinity to both phases, which can strongly modify the morphology, interfacial adhesion, and

* Corresponding author. Tel.: +54 291 4861700x283; fax: +54 291 4861600.
E-mail address: sbarbosa@plapiqui.edu.ar (S.E. Barbosa).

0032-3861/$ - see front matter © 2007 Elsevier Ltd. All rights reserved.
doi:10.1016/j.polymer.2006.12.040

final mechanical properties of the blend. The effectiveness of polymer–polymer compatibilization also depends on the architecture (structure and molecular weight) of the interfacial agent. If the copolymer tends to entangle with the homopolymer phases by the presence of long ''loops'', these can expand into the homopolymer phases and favor the strengthening of the interphase [10]. Several authors have published about the influence of architecture of block copolymers in addition compatibilization of immiscible blends. It was found that the interfacial strength depends on the adequate combination of block length and distribution [11–13]. However, much less attention was devoted to in situ compatibilization, probably due to the difficulty inherent to the reaction products analysis [14].

In previous works [15–17], Friedel–Crafts alkylation reaction (F–C) was carried out in molten state onto polyolefin/PS blends in order to compatibilize them, but neither the interfacial aspects nor the effect of molecular weights (MW) on compatibilization efficiency and the effect of the catalyst system on the pure resins were assessed.

In our previous work, F–C alkylation reaction was used to graft polyethylene (PE) chains, having two different MW, onto polystyrene (PS) to obtain the corresponding copolymer PE-*g*-PS. The relation between the initial PE MW and the structure of the copolymer obtained was analyzed by a combination of size exclusion chromatography (SEC) and Fourier Transform Infrared Spectroscopy (FTIR). The relative lengths of the grafted PE chains were assessed, having found that the longer the PE chains, the lower the grafting density. Secondary reaction occurrence was also investigated and it was demonstrated that PE does not suffer any change in MW upon reaction, while PS presents chain scission at high catalyst contents. In addition, neither PE nor PS crosslinking evidences were detected [18].

In the present work, the F–C reaction was applied, as reactive compatibilization method, for PE/PS blends. Two polyethylenes with different molecular weights and the same PS were used along a wide range of catalyst concentration. The influence of the graft copolymer architecture and content on the efficiency of blend compatibilization was studied. The emulsifying effect, morphological aspects and mechanical behavior were also assessed for these blends.

2. Experimental

2.1. Materials

2.1.1. Homopolymers

Polystyrene (PS) Lustrex HH-103 (M_w: 270 600 g/mol, M_n: 136 000 g/mol) was supplied by UNISTAR S.A. Two grades of linear low-density polyethylene came from Dow-Polisur, LLDPE 6200 (M_w: 52 000 g/mol, M_n: 16 700 g/mol) and 6500 (M_w: 40 000 g/mol, M_n: 11 000 g/mol), further on called PE62 and PE65, respectively.

2.1.2. Catalyst

The catalyst system for the F–C reactions was anhydrous aluminum chloride ($AlCl_3$) (>98% purity) from Merck, with 0.3 wt% styrene (St) (>99% purity). The catalyst was wetted in *n*-hexane to protect it from air moisture.

2.2. Blending

2.2.1. Physical blends

Two sets of PE (80 wt%)/PS (20 wt%) physical blends were prepared. They were called PB62 and PB65, for PE62 and PE65, respectively. The blends were made, under nitrogen atmosphere, in a batch mixer (Brabender Plastograph W50) at 190 °C. Table 1 summarizes the characteristics of the blends prepared. The mixing procedure includes the initial melting of PS, and subsequent incorporation of PE under nitrogen. Mixing of PB62 was carried out at 30 rpm during 12 min, while the PB65 was processed at 50 rpm during 20 min. The mixer conditions were adjusted to reach the same PE/PS viscosity ratio and dispersion degree for each blend.

2.2.2. Reactive blends and reactive homopolymers

The reaction was carried out in the same batch mixer and at the same temperature, speed and time as used for the physical blends. In all cases the F–C reaction was performed after the complete melting and mixing was reached. The 0.3 wt% styrene was added, followed by 0.1, 0.3, 0.7, 1.0 and 1.5 wt% $AlCl_3$. The resulting reactive blends were named RB62 and RB65 (Table 1). In the same way, the reactive homopolymers were named RPE62 and RPE65 followed by the catalyst content.

2.3. High-pressure high-temperature solvent extractions

A novel method based on high-pressure high-temperature solvent extraction, which is described in Ref. [19], was used for copolymer quantification. The reactive blend extractions were carried out simultaneously with the corresponding physical blends to assure equal process conditions. About 50 mg of each blend was confined in each sample holder with a Teflon microporous filter, and introduced into the 10 cm^3 cylindrical cell. Then, the cylinder was pressurized to 30 MPa and the temperature increased to 140 °C. The extraction time was 1 h keeping the solvent flow rate at 40 cm^3/h. The blend

Table 1
Nomenclature and concentrations of all blends prepared

Abbreviation	LLDPE	PE/PS [wt%]	$AlCl_3$ [wt%][a]	St [wt%][a]
Physical blends				
PB62	6200	80/20	0	0
PB65	6500	80/20	0	0
Reactive blends				
RB62 0.1	6200	80/20	0.1	0.3
RB62 0.3	6200	80/20	0.3	0.3
RB62 0.5	6200	80/20	0.5	0.3
RB62 0.7	6200	80/20	0.7	0.3
RB62 1.0	6200	80/20	1.0	0.3
RB62 1.5	6200	80/20	1.5	0.3
RB65 0.3	6500	80/20	0.3	0.3
RB65 1.0	6500	80/20	1.0	0.3

[a] Weight percent calculated over 100% of blend mass.

components were separated by sudden solvent expansion and subsequent collection of the soluble fraction.

2.4. Blend morphology

The blend morphology was analyzed in a JEOL 35 CF scanning electron microscope equipped with secondary electron detection. The samples were fractured under liquid nitrogen and the fracture surfaces coated with Au in a vacuum chamber. Analysis PRO™ software was used for processing the particle size data. About 300 particles were considered to calculate the average particle diameter of the disperse phase (Dp) and its standard deviation, σ(Dp).

2.5. Tensile tests

Tensile tests were carried out at room temperature in an Instron tester with crosshead speed of 5 mm/min. Dog-bone shaped tensile specimens were cut from plates prepared by compression molding. The bone specimen dimensions were scaled down to one third of ASTM D638M norm dimensions (specimen type IV).

2.6. Characterization

2.6.1. Gel permeation chromatography (GPC)

The weight-average molar mass (M_w) of pure and reactive homopolymers was obtained in a Waters Scientific chromatograph model 150-CV. The different samples were dissolved in 1,2,4-trichlorobenzene (0.0125 wt% BHT) at the same initial concentration and then injected at 135 °C.

2.6.2. Fourier transform infrared spectroscopy (FTIR)

All samples prepared were checked by FTIR looking for oxidation peaks (1700 cm^{-1}). No peak appeared in this zone, indicating that this compatibilization does not cause any oxidative process. Also, the composition homogeneity of the blends in the bulk was estimated by comparing the ratio of characteristic IR absorption peaks of each homopolymer. A detailed description of this technique is reported in Ref. [18].

3. Results and discussions

3.1. Chemical aspects

The F–C reaction occurrence and the PE-*g*-PS copolymer formation for the PE/PS blends studied were proved in a previous work [18]. According to thermodynamic and kinetic theoretical studies, the shorter polymer chains are located at the interphase [20–23]. Then, it can be expected that the F–C alkylation reaction between PE and PS, which takes place at the interphase, involves mainly short chain molecules.

In order to check the possible occurrence of secondary reactions, originated by the catalyst system, the F–C reaction was carried out on the homopolymers. The same catalyst concentrations and reaction conditions as for reactive blends were used. The results are summarized in Table 2.

Table 2
Average molecular weights for homopolymers and reactive homopolymers (RPE62, RPE65 and RPS)

Reactive PE	M_w [g/mol]	Reactive PS	M_w [g/mol]
PE62	50 700	PS	256 000
RPE62 0.1	50 200	RPS 0.1	257 300
RPE62 0.3	50 800	RPS 0.3	248 000
RPE62 0.5	49 900	RPS 0.5	243 000
RPE62 0.7	50 000	RPS 0.7	194 000
RPE62 1.0	49 400	RPS 1.0	25 700
RPE62 1.5	50 500	RPS 1.5	<20 000[a]
PE65	39 000		
RPE65 0.3	39 200	RPS 0.3	250 000
RPE65 1.0	38 000	RPS 1.0	<20 000[a]

RPS was prepared under PE62 and PE65 processing conditions and it is listed next to the corresponding RPE.
[a] Out of the limit of detection of the GPC columns used.

It is observed that the reaction does not produce any MW variation in both PEs, indicating absence of crosslinking or chain scission secondary reactions. On the other hand, PS MW remains constant at low catalyst concentration, but it suffers important drops at $AlCl_3$ concentrations higher than 0.5 wt%, falling to one tenth of the original value when 1.0 wt% $AlCl_3$ is used. Therefore, at high catalyst concentration, F–C reaction coexists with PS chain scission. These results will be taken into account in the copolymer quantification as well as in the final properties determination of the compatibilized blends.

3.2. Graft copolymer quantification

From PE/PS physical blends, the entire PE phase was solubilized by *n*-heptane at near critical pressure and temperature. For the corresponding reactive blends, containing PE-*g*-PS in addition to PE and PS, the copolymer was solubilized, as a result of chemical affinity, along with the PE phase [19]. Both, the soluble and insoluble fractions were analyzed by GPC and FTIR. The soluble fraction contained the unreacted PE phase, as well as the copolymer formed while the insoluble phase was only PS. The difference between the original PS mass in the blend (20 wt%) and the PS mass remaining in the insoluble phase corresponds to the PS grafted. This quantity can be expressed as percentage of grafted PS (PS_g) referred to the original PS mass in the blend. The PS_g as a function of catalyst concentration, for both sets of reactive blends, is shown in Fig. 1. When catalyst concentration is low (0.3 wt%), a different reaction yield is observed for each set; while for high catalyst content (1.0 wt%) PS_g is the same for both sets. For an adequate assessment of results, these two zones are analyzed independently.

3.2.1. Low $AlCl_3$ content

Table 2 shows clearly that, at low catalyst concentration, neither chain scission nor crosslinking reactions occur, so the only difference between the two sets of reactive blends is the MW of PE62 and PE65. Nevertheless, a much higher reactivity was determined for RB65 than for RB62. At

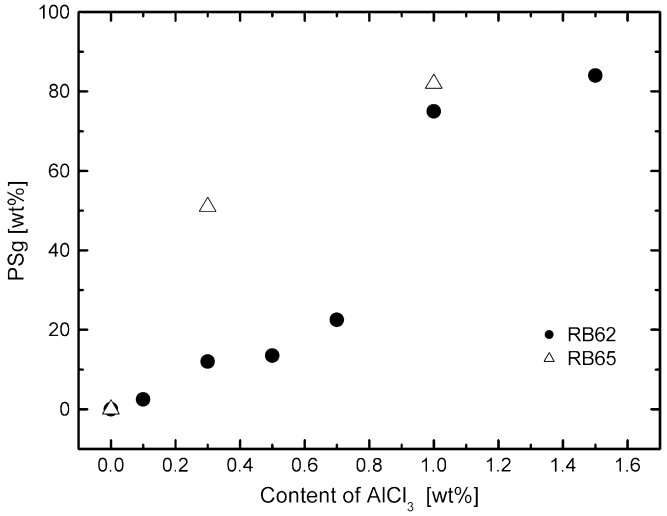

Fig. 1. PS content in the copolymer (PS_g) as a function of the amount of $AlCl_3$, for both sets of reactive blends (RB62 and RB65).

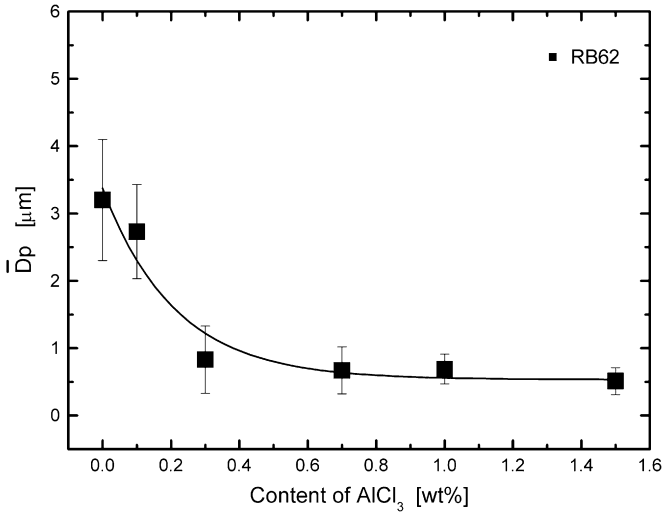

Fig. 2. Emulsification curve for RB62: average diameter particle (Dp) as a function of catalyst content. Plane line corresponds to exponential fit.

0.3 wt% $AlCl_3$, RB62 (longer PE chain) contains 15 wt% PS_g, while RB65 (shorter PE chain) has 50 wt% PS_g. This difference may be explained by the fact that lower MW fractions of components are located at the interphase [20]. In this sense, the theories for predictions of copolymer reactions, in molten state between two immiscible homopolymers, arrive at similar conclusion [23,24]. Particularly, Kramer predicts that the grafting density of brush copolymer decreases with the polymerization degree. Then, low MW chains are more reactive due to their greater mobility.

3.2.2. High $AlCl_3$ content

Fig. 1 shows that both reactive blend sets exhibit a sharp increase in PS_g. The RB62 presents such increase in reactivity at high catalyst content (1.0 wt%), suggesting that this is originated in the PS MW decrease due to chain scission (Table 2) and the consequent increase in chain mobility. In contrast, for RB65 this effect is observed at very low catalyst concentrations (0.3 wt%), and can be attributed to a higher reactivity of their shorter chain lengths.

3.3. Emulsifying effect

As the F–C reaction occurs at the same interphase that needs to be compatibilized, the copolymer formed works as a tailor-made compatibilizer due to the high physical–chemical affinity between the components. Then, an interfacial tension and consequently particle size (Dp) reduction can be expected. For both sets of blends, the emulsification curves were built as average particle diameter as a function of catalyst content (Figs. 2 and 3). These curves present the classical behavior reported by many authors for the compatibilization of immiscible polymer blends [25–27]. Both blend sets show a remarkable emulsifying effect, reaching important Dp drops, even at very low catalyst contents. After this decrease, Dp remains constant indicating that the critical micelle concentration (cmc) is reached and the interphase is saturated with the copolymer. It is noted that even if the cmc is the same for both blends (0.3 wt% $AlCl_3$), the PS_g is very different (Fig. 1). The amount of PE65-*g*-PS is three times higher than that of PE62-*g*-PS. These results are consistent with the Noolandi theory [28], in which the reduction of interfacial tension due to a high concentration of low MW copolymer is similar to that achieved with a low concentration of high MW copolymer.

3.4. Morphological aspects

The morphology of the blends was studied by SEM of cryogenic fractured surfaces. The shape and homogeneity of the dispersed phase, as well as the type of fracture were analyzed. Fig. 4 shows micrographs of fractured surfaces from both physical blends. Particles of PS and the holes left by them during the fracture process can be observed. The fracture is

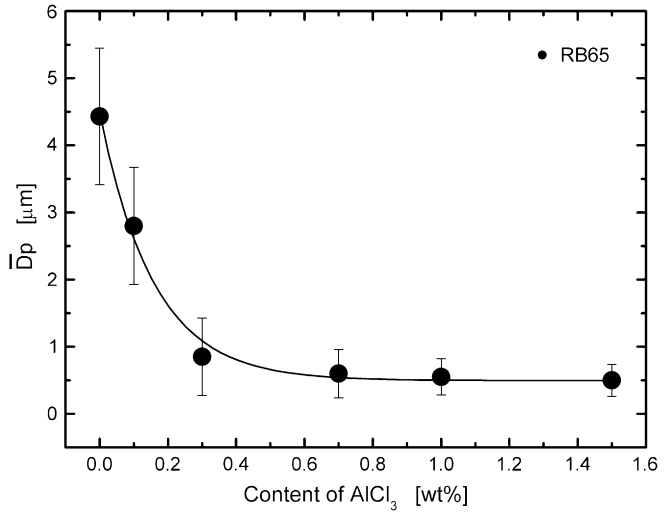

Fig. 3. Emulsification curve for RB65: average diameter particle (Dp) as a function of catalyst content. Plane line corresponds to exponential fit.

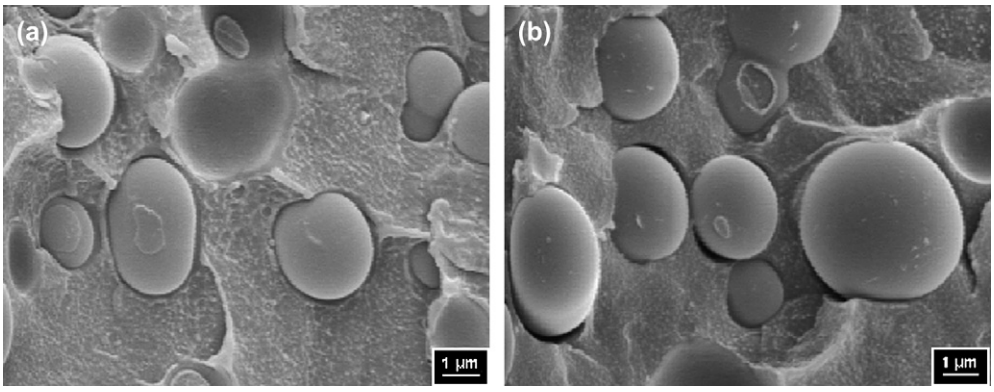

Fig. 4. Micrographs for (a) PB62 and (b) PB65.

clearly inter-particle and the borders are detached. In contrast, the compatibilized blends, with 0.3 wt% catalyst, exhibit a trans-particle fracture (Fig. 5). This change in the fracture mode, resulting from the compatibilization reaction, would be consistent with an improvement in interfacial adhesion.

A considerable decrease in particle size, as well as a different type of fracture is observed as compared to the physical blends. The particles and matrix appear fractured along the same plane (trans-particle fracture) proving a high interfacial adhesion. The increment in adhesion is more pronounced for reactive blends with 1.0 wt% of catalyst as it is shown in Fig. 6. Also, a large reduction in Dp and its dispersion is observed, which is in agreement with the emulsifying effect presented above.

In Figs. 5a and 6a, for RB62, the effect of some elastic chain shrinking after fracture, leading to ring shaped edges around the particles can be appreciated. These edges, which are more prominent for RB62 1.0 than for RB62 0.3, possibly contain more elastic copolymer material, elongated during the fracture process and retracted afterwards. During the fracture process, the molecules suffer first a pulling (stretching), and after blend fracture an elastic shrinking (when room temperature is reached). These steps are represented in the scheme of Fig. 7. Also, the longer grafted chains would present a more remarkable effect. The appearance of these ring edges in RB62 micrographs can be related to the cmc and the length of the grafted PE62 chains as follows. Before the F–C reaction starts, the shorter homopolymer molecules are located preferably at the interphase, being the most reactive ones [21–23]. As the reaction progresses, homopolymer molecules are spent in copolymer formation. When the copolymer concentration at the interphase reaches cmc, a renewal process starts to occur. Copolymer migrates to the bulk and new homopolymer to the interphase so that the last molecules consumed and formed are longer than the initial ones [29]. Now, for RB62 1.0 the cmc is largely exceeded and interfacial copolymer molecules are expected to have longer PE grafted chains than the ones for RB62 0.3; therefore more marked ring edges appear in RB62 1.0. In this sense, this trend is also evident when different MW reactive blends, for the same catalyst content, are compared (Fig. 6a and b).

3.5. Mechanical behavior

The tensile test behavior of the physical and reactive blends, as well as their corresponding homopolymers, is studied. In assessing the compatibilization effect on the tensile properties, the elongation at break (ε_b) was selected as a representative property. It involves large deformations, then is related to the interfacial adhesion and gives information about interfacial strength [30]. The yield behavior can also give qualitative information on the compatibilization state, particularly when the changes in adhesion between compatibilized and PB are large. In contrast, the elastic modulus is less sensitive to compatibilization effects because it is a quasi-zero

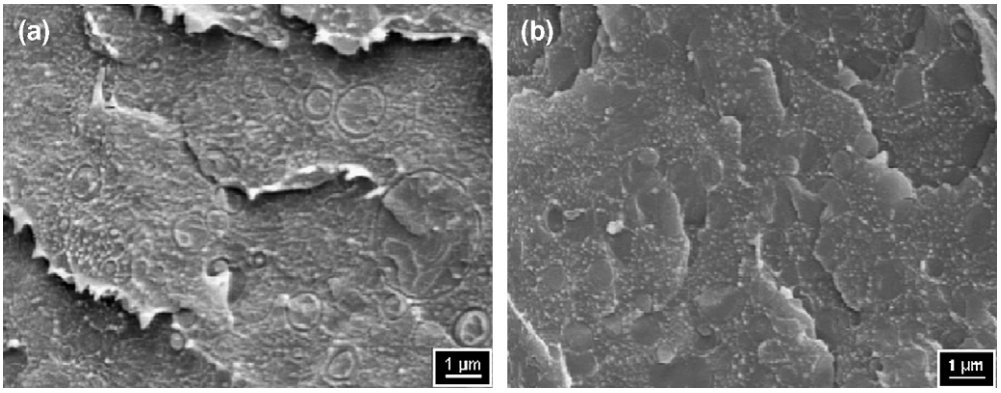

Fig. 5. Micrographs for (a) RB62 0.3 and (b) RB65 0.3.

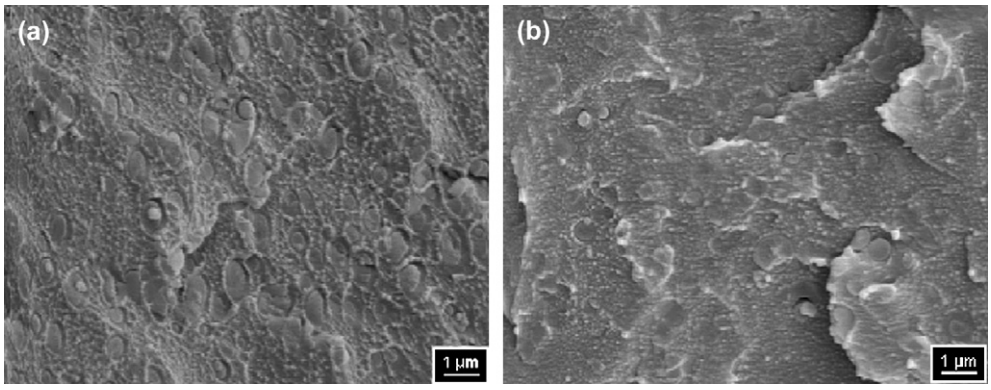

Fig. 6. Micrographs for (a) RB62 1.0 and (b) RB65 1.0.

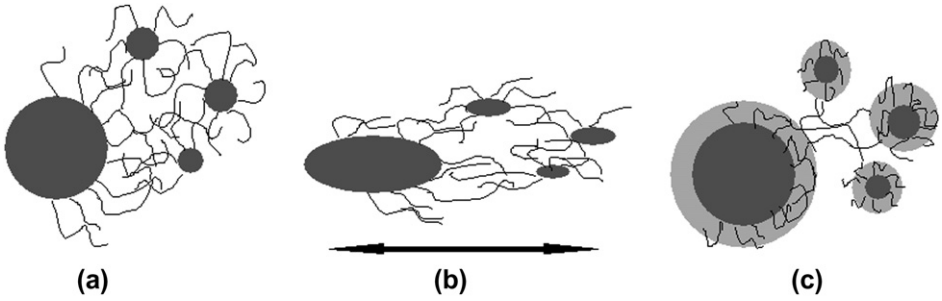

Fig. 7. Scheme for cryogenic fracture process of reactive blends: (a) initial state, (b) stretching during fracture and (c) shrinking after fracture, at room temperature.

strain property and depends more on the inherent composition of the blend.

For blends based on crystallizable matrices, the mechanical properties also depend on the crystalline state (crystallinity degree, distribution of crystal sizes, morphology of crystalline structures, etc.). So, in order to properly compare compatibilization effects through mechanical properties, the possible changes in crystalline parameters must be assessed. Fig. 8 shows the DSC thermograms of pure PE62 and the PB62 and RB62. The peak melting temperatures of PE and blends are very close to each other, only a minor reduction in peak broadness of the blends, with respect to the pure PE, is observed. Analogous results were obtained with PE65, PB65 and RB65, allowing to assume that the crystalline structure is not affected by the presence of the compatibilizer. Other authors reported for this system, that compatibilizer only reduces the dispersed phase particle size, but does not have any effect on the crystalline morphology [31].

Tensile tests were performed on homopolymers, physical blends and 0.3 and 1.0 wt% catalyst reactive blends. Fig. 9 shows the stress–strain behavior of PE65 blends. PB65

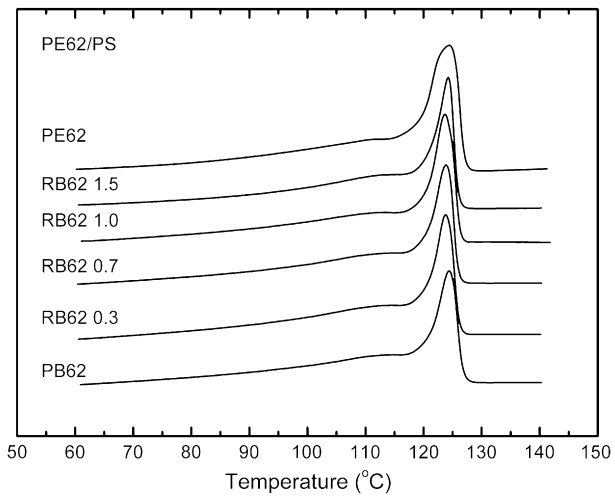

Fig. 8. DSC thermograms of pure PE62, physical and reactive PE62/PS blends.

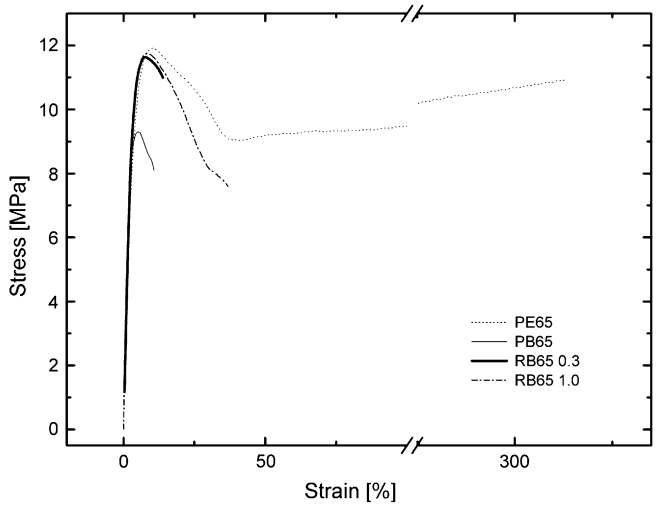

Fig. 9. Stress–strain curve, tensile test for PE65, PB65 and RB65 with 0.3 and 1.0 wt% of catalyst.

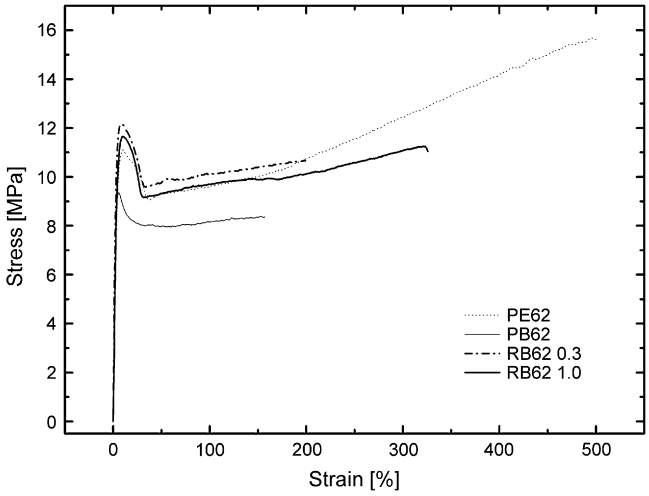

Fig. 10. Stress–strain curve, tensile test for PE62, PB62 and RB62 with 0.3 and 1.0 wt% of catalyst.

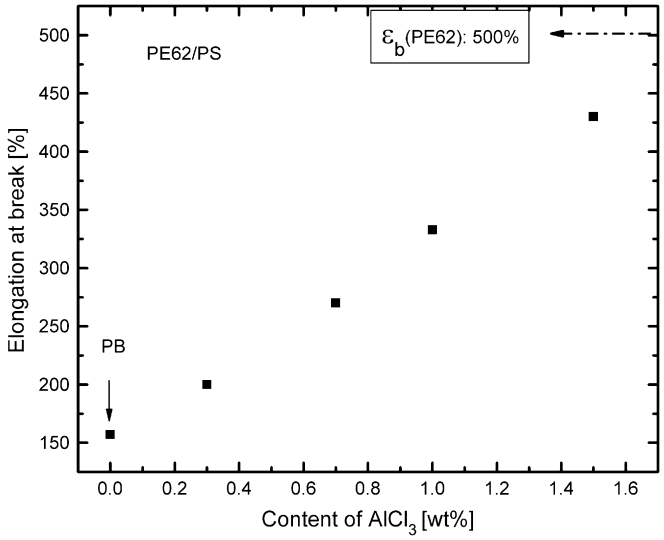

Fig. 11. Elongation at break, tensile test, for all RB62 prepared and PB62.

exhibits an ε_b about 20% lower than PE65. It can be explained by the addition of 20 wt% PS which is more brittle than PE. Moreover, despite that all the blends fracture before necking, indicating low ductility, the reactive blends show higher ε_b than the physical ones. The yield behavior can also give qualitative information on the compatibilization state. The physical blend has yield strength approximately 20% less than pure PE65. On the contrary, reactive blends present slightly greater yield strengths than the matrix. This can be explained taking into account the lack of continuity between PE and PS phases in the physical blends (Fig. 4). During the tensile test, only the continuous PE phase (which is about 80% in volume) resists the load. On the other hand, the behavior of reactive blends is different. First, all the blends tested were at or above the cmc. It means that the interphase is saturated with copolymer and therefore compatibilized. The copolymer molecules are entangled with both phases anchoring them. Now, during the tensile test, both phases contribute to the strength resulting in slightly higher yield point than for pure PE.

In Fig. 10, stress–strain curves for the set of PE62 blends are presented. Also, for PB62 a remarkable ε_b decrease is observed in comparison with PE62, and the explanation is again the addition of 20 wt% PS. RB62 0.3 presents an increase of ε_b with respect to PB62, and this increment is more pronounced for RB62 1.0, showing that the copolymer improves the interphase adhesion at both low and high catalyst contents. It is clear from Fig. 10 that yield strength for PE62 blends follows a similar behavior as for PE65 blends, decreasing for PB62 and increasing for RB62.

In order to study the compatibilization effect on the mechanical behavior in more detail, the tensile tests were carried out on RB62 for a wide range of catalyst contents. Fig. 11 shows a significant quasi-linear increment in ε_b with $AlCl_3$. Even for very low catalyst concentration (e.g. 0.3 wt%), ε_b increases about 25% with respect to PB and for high catalyst concentration (e.g. 1.5 wt%) ε_b becomes nearly three times higher. At this high $AlCl_3$ concentration ε_b is close to the ε_b of PE62. Considering that ε_b increases even for blends that are far above the cmc condition, the crystalline structure remains unchanged and neither chain scission nor crosslinking reactions occur, the possible causes for this continuous ε_b increase should be assigned to interphase modifications due to PE grafted chain lengths. The observed increase in ductility can be interpreted in terms of entanglement molecular weight (M_c) and its variation with the catalyst concentration. The PE62 exhibits a significant fraction of molecules with chain lengths equal to or greater than the M_c of PE (4000 to ~30 000 g/mol) [18,32]. As it was discussed in Section 3.2, the shorter molecules tend to move with priority to the interphase, reacting in first place. Now, when the saturation concentration is exceeded, the copolymer is forced to leave the interphase, driven by both thermodynamic and shear forces [28,33]. Afterwards, new copolymer will be produced from longer homopolymer molecules, whenever catalyst remains at the interphase. So, the RB62 1.5 should have higher MW copolymer (capable to form better developed entanglements) at the interphase than the RB62 0.3. Therefore, the entanglements in RB62 1.5 would be stronger than in RB62 0.3, leading to greater elongation at break.

4. Conclusions

From this study, the following conclusions regarding the effect of the in situ copolymer architecture and content on the efficiency of the reactive compatibilization of PE/PS blends are obtained.

- The amount of copolymer formed increases with the catalyst concentration and the short chain length fraction of the homopolymers.
- The cmc was reached either with 50% long chain graft copolymer (RB62) and 17% short chain graft copolymer (RB65) using, in any case, a very low catalyst concentration (0.3 wt%). In this sense, longer chain length copolymers behave as more efficient compatibilizers for these blends.

- The length of the grafted PE chains plays an important role in interfacial adhesion. Long chain grafts make more effective entanglements with the PE matrix. According to the dynamics of the reaction at the interphase, longer chain copolymer is formed as the catalyst concentration increases. In correspondence, a greater interfacial adhesion can be expected for higher catalyst content.
- The copolymer formed by in situ F–C reaction on PE/PS blends showed a notorious compatibilizing effect. A substantial increase in interfacial adhesion and particle size reduction was achieved even at catalyst concentrations as low as 0.3 wt%.
- For the higher MW PE blends the interfacial strength is considerably enhanced by compatibilization. The elongation at break increases linearly with the catalyst content, from 25% (0.3 wt% catalyst) to 300% (1.5 wt% catalyst) with respect to physical blend, even though the blends include 20 wt% of a brittle component (PS).

Acknowledgments

Financial support from CONICET (National Research Council of Argentina), SECyT (Secretary of Science, Technology and Productive Innovation of Argentina) and UNS (National University of the South) is acknowledged.

References

[1] Pukanszky B. Eur Polym J 2005;41:645–62.
[2] Utracki LA. Introduction. In: Utracki LA, editor. Polymer blends handbook, vol. 1. Netherlands: Kluwer Academic Publishers; 2002. p. 1–121.
[3] Datta S, Lohse D. Polymeric compatibilizers. Munich: Hanser; 1996. Part A.
[4] Utracki LA. Polymer alloys and blends. Munich: Hanser; 1989 [chapter 1].
[5] Bisio AT, Xantos M. How to manage plastics waste: technology and market opportunities. Munich: Hanser; 1995 [chapter 1].
[6] Utracki LA. Two-phase polymer systems. Munich: Hanser; 1991 [chapter 7].
[7] Majumdar B, Paul D. Reactive compatibilization. In: Paul DR, Bucknall CB, editors. Polymer blends, vol. 1. New York: John Wiley; 2000. p. 539–79.
[8] Pagnoulle C, Koning C, Leemans L, Jerome R. Macromolecules 2000; 33:6275–83.
[9] Majumdar B, Keskkula H, Paul D, Harvey N. Polymer 1994;35(20): 4263–79.
[10] Eastwood E, Viswanathan S, O'Brienc CP, Kumar D, Dadmun MD. Polymer 2005;46:3957–70.
[11] Macaúbas P, Demarquette N. Polymer 2001;42:2543–54.
[12] Halimatudahliana, Ismail H, Nasir M. Polym Test 2002;21:163–70.
[13] Kim S, Kim JK, Park CE. Polymer 1997;38:1809–15.
[14] Brown SB. In: Utracki LA, editor. Polymer blends handbook, vol. 1. Netherlands: Kluwer Academic Publishers; 2002. p. 339–416.
[15] Sun Y, Baker WE. J Appl Polym Sci 1997;65:1385–93.
[16] Sun Y, Willemse JG, Liu TM, Baker WE. Polymer 1998;39(11):2201–8.
[17] Gao Y, Huang H, Yao Z, Shi D, Ke Z, Yin J. J Polym Sci Part B Polym Phys 2003;41:1837–49.
[18] Diaz M, Barbosa S, Capiati N. Polymer 2002;43(18):4851–8.
[19] Barbosa S, Diaz M, Mabe G, Brignole E, Capiati N. J Polym Sci Part B Polym Phys 2005;43:2361–9.
[20] Helfand H, Tagami K. Polym Lett 1971;9:741–6.
[21] Hong K, Noolandi J. Macromolecules 1982;15:482–92.
[22] Hong K, Noolandi J. Macromolecules 1981;14:727–36.
[23] Kramer EJ. Isr J Chem 1995;35:49–54.
[24] O'Shaughnessy B, Sawhney U. Macromolecules 1996;29:7230–9.
[25] Favis BD. Factors influencing the morphology of immiscible polymer blends in melt processing. In: Paul DR, Bucknall CB, editors. Polymer blends, vol. 1. New York: John Wiley; 2000. p. 501–38.
[26] Li J, Favis BD. Polymer 2002;43:4935–45.
[27] Willis JM, Favis BD. Polym Eng Sci 1990;30:1073–84.
[28] Noolandi J. Polym Eng Sci 1984;24(2):70–8.
[29] Díaz M. Compatibilización de Mezclas de PE, PP y PS. Aplicación de la Reacción de Alquilación de Friedel–Crafts. Ph.D. thesis, Universidad Nacional del Sur (UNS), Argentina; 2004.
[30] Nielsen LE, Landel RF. Mechanical properties of polymers and composites. New York: Dekker; 1994.
[31] Kim T, Kim D, Kim W, Lee T, Suh K. J Polym Sci Part B Polym Phys 2004;42(15):2813–20.
[32] Sperling LH. Polymeric multicomponent materials. New York: Wiley; 1997 [chapter 6].
[33] Pan L, Inoue T, Hayami H, Nishikama S. Polymer 2002;43:337–43.